

Quark Stars as inner engines for Gamma Ray Bursts?

Rachid Ouyed and Francesco Sannino

Nordic Institute for Theoretical Physics, Blegdamsvej 17, DK-2100 Copenhagen, Denmark

Received/Accepted

Abstract. A model for Gamma ray bursts inner engine based on quark stars (speculated to exist in nature) is presented. We describe how and why these objects might constitute new candidates for GRB inner engines. At the heart of the model is the onset of exotic phases of quark matter at the surface of such stars, in particular the 2-flavor color superconductivity. A novel feature of such a phase is the generation of particles which are unstable to photon decay providing a natural mechanism for a fireball generation; an approach which is fundamentally different from models where the fireball is generated during collapse or conversion of neutron star to quark star processes. The model is capable of reproducing crucial features of Gamma ray bursts, such as the episodic activity of the engine (multiple and random shell emission) and the two distinct categories of the bursts (two regimes are isolated in the model with ~ 2 s and ~ 81 s burst total duration).

Key words. dense matter – Gamma rays: bursts – stars: interior

1. Introduction

A central problem contributing to the Gamma-ray bursts (GRBs) mystery is the unknown nature of the engine powering them (Kouveliotou et al. 1995; Kulkarni et al. 1999; Piran 1999a; Piran 1999b). Many have been suggested but it is fair to say that we are still far from a definite answer. Regardless of the nature of the engine, however, it is widely accepted that the most conventional interpretation of the observed GRBs result from the conversion of the kinetic energy of ultra-relativistic particles to radiation in an optically thin region. The particles being accelerated by a fireball mechanism (or explosion of radiation) taking place near the central engine (Goodman 1986; Shemi & Piran 1990; Paczyński 1990).

The first challenge is to conceive of circumstances that would create a sufficiently energetic fireball. Conversion of neutron stars to quark stars (Olinto 1987; Cheng & Dai 1996; Bombaci & Datta 2000) has been suggested as one possibility. Other models also involve the compact object element; such as black holes (Blandford & Znajek 1977) and coalescing neutron stars (Eichler et al. 1989; Ruffert & Janka 1999; Janka et al. 1999). We show in this work that the plausible existence of quark stars combined with the onset of a newly revived state of quark matter - called color superconductivity - in these objects offers a new way of tackling the GRB puzzle (Ouyed 2002). Here we will argue that quark stars might constitute new candidates for GRB inner engines.

Quark matter at very high density is expected to behave as a color superconductor (see Rajagopal & Wilczek 2000 for a review). Associated with superconductivity is the so-called gap energy Δ inducing the quark-quark pairing and the critical temperature (T_c) above which thermal fluctuations will wash out the superconductive state. A novel feature of such a phase is the generation of glueball like particles (hadrons made of gluons) which as demonstrated in Ouyed & Sannino (2001) immediately decay into photons. If color superconductivity sets in at the surface of a quark star the glueball decay becomes a natural mechanism for a fireball generation.

The paper is presented as follows: In Sect. 2 we briefly describe the concept of color superconductivity in quark matter. Glueball formation and their subsequent two-photon decay is described. Sect. 3 deals with quark stars and the onset of color superconductivity at their surface. In Sect. 4, we explain how GRBs are powered in this picture and show that variability (multiple shell emission) is inherent to the inner engine. We isolate two GRB regimes in Sect. 5 associated with small and massive quark stars. The model's features and its predictions are summarized in Sect. 6 while a discussion and conclusion follows in Sect. 7 where the model's assumptions and limitations are highlighted.

2. Color Superconductivity

While in this paper we deal mostly with the astrophysics aspect of the model, we nevertheless give a brief overview of color superconductivity and the glueball-to-photon de-

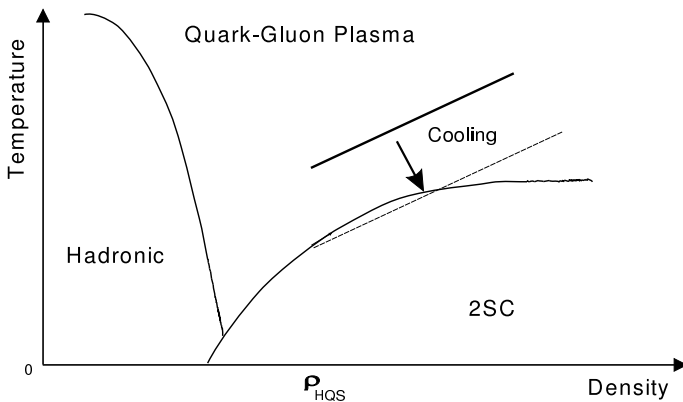


Fig. 1. A schematic representation of a possible QCD phase diagram (Rajagopal & Wilczek 2000). At high temperature and density, matter is believed to be in a quark-gluon plasma phase (QGP). The hadronic phase lies in the region of low temperature and density. At very high density but low temperature, when nuclei melt into each other, it has been suggested that a color superconductive phase might set in. 2SC denotes a 2-flavor color superconductive regime. The arrow depicts a plausible cooling path of a HQS surface leading to the onset of color superconductivity.

cay process which leads to the fireball. The interested reader is referred to Ouyed & Sannino (2001) for the underlying physics. For a recent review see Sannino (2002)

2.1. 2-flavour color superconductivity

A reasonable Quantum Chromo-Dynamics (QCD) phase diagram (in the μ - T plane, where μ is the chemical potential simply related to matter density) is shown in Fig. 1. At high temperature and density, matter is believed to be in a quark-gluon plasma phase (QGP). The hadronic phase lies in the region of low temperature and density. At high densities but low temperatures, when nuclei melt into each other, it is now believed that a color superconductive phase sets in. This phase is characterized by the formation of quark-quark condensate. In the 2-flavor color superconductivity (2SC) the up and down quark come into play during pairing. Furthermore, 2SC is characterized by five out of the eight gluons acquiring mass. We refer the interested reader to Rajagopal & Wilczek (2000) for a review of the dynamical properties of 2SC.

2.2. Light GlueBalls

The 3 massless gluons in the 2SC phase which bind into light glueballs (LGBs) together with the quarks up and down constitute the 2SC phase mixture. In Ouyed & Sannino (2001) we studied certain properties of these LGBs. Among the properties relevant to our present study we found, i) The LGBs decay into photons with an associated lifetime of the order of 10^{-14} s; ii) The mass of the LGBs is of the order of 1 MeV.

3. Quark stars

We now turn to study the astrophysical consequences when such a state sets in at the surface of quark stars. As such, we first assume that quark stars exist in nature (further discussed in Sect. 7.1) and constitutes the first major assumption in our model.

3.1. Hot Quark stars

We are concerned with quark stars born with surface temperatures above T_c . We shall refer to these stars as “hot” quark stars (HQSS) in order to avoid any confusion with strange stars which are conjectured to exist even at zero pressure if strange matter is the absolute ground state of strong interacting matter rather than iron (Bodmer 1971; Witten 1984; Haensel et al. 1986; Alcock et al. 1986; Dey et al. 1998).

We borrow the language of the MIT-bag model formalism at low temperature and high density to describe HQSS (Farhi & Jaffe 1984). This gives a simple equation of state

$$P = b(\rho - \rho_{\text{HQS}})c^2, \quad (1)$$

where b is a constant of model-dependent value (close to, but generally not equal, to 1/3 of the MIT-bag model), and ρ_{HQS} is the density at zero-pressure (the star’s surface density). We should keep in mind that $T_c/\mu \ll 1$ as is confirmed later.

Features of HQSS are - to a leading order in T_c/μ - identical to that of strange stars. The latter have been studied in details (Alcock et al. 1986; Glendenning & Weber 1992; Glendenning 1997). Of importance to our model:

i) The “surface” of a HQS is very different from the surface of a neutron star, or any other type of stars. Because it is bound by the strong force, the density at the surface changes abruptly from zero to ρ_{HQS} . The abrupt change (the thickness of the quark surface) occurs within about 1 fm, which is a typical strong interaction length scale.

ii) The electrons being bound to the quark matter by the electro-magnetic interaction and not by the strong force, are able to move freely across the quark surface extending up to $\sim 10^3$ fm above the surface of the star. Associated with this electron layer is a strong electric field (5×10^{17} V/cm)- higher than the critical value (1.3×10^{16} V/cm) to make the vacuum region unstable to spontaneously create (e^+ , e^-) pairs.

iii) The presence of normal matter (a crust made of ions) at the surface of the quark star is subject to the enormous electric dipole. The strong positive Coulomb barrier prevents atomic nuclei bound in the nuclear crust from coming into direct contact with the quark core. The crust is suspended above the vacuum region.

iv) One can show that the maximum mass of the crust cannot exceed $M_{\text{crust}} \simeq 5 \times 10^{-5} M_{\odot}$ set by the requirement that if the density in the inner crust is above the neutron drip density ($\rho_{\text{drip}} \simeq 4.3 \times 10^{11}$ g/cc), free neutrons will gravitate to the surface of the HQS and be converted

to quark matter. This is due to the fact that neutrons can easily penetrate the Coulomb barrier and are readily absorbed.

3.2. Cooling and 2SC layer formation

The HQS surface layer might enter the 2SC phase as illustrated in Fig. 1. In the QCD phase diagram (Fig. 2), (ρ_{B_0}, T_{B_0}) is the critical point beyond which one re-enters the QGP phase (the extent of the 2SC layer into the star). The star consists of a QGP phase surrounded by a 2SC layer where the photons (from the LGB/photon decay) leaking from the surface of the star provides the dominant cooling source. This picture, as illustrated in Fig. 2, is only valid if neutrino cooling in the 2SC phase is heavily suppressed as to become slower than the photon cooling. Unfortunately, the details of neutrino cooling in the 2SC phase is still a topic of debate and studies (Carter & Reddy 2000; Schaab et al. 2000 to cite only few). One can only assume such a scenario which constitutes the second major assumption in our model. In Sect. 7.2, we discuss the remaining alternative when photon cooling is dwarfed by neutrino cooling.

3.3. LGBs decay and photon thermalization

The photons from LGB decay are generated at energy $E_\gamma < T_c$ and find themselves immersed in a degenerate quark gas. They quickly gain energy via the inverse Compton process and become thermalized to T_c . We estimate the photon mean free path to be smaller than few hundred Fermi (Rybicki & Lightman 1979; Longair 1992) while the 2SC layer is measured in meters (see Sect. 5.2). A local thermodynamic equilibrium is thus reached with the photon luminosity given by that of a black body radiation,

$$L_\gamma = 3.23 \times 10^{52} \text{ ergs s}^{-1} \left(\frac{R_{\text{HQS}}}{5 \text{ km}}\right)^2 \left(\frac{T_c}{10 \text{ MeV}}\right)^4. \quad (2)$$

The energy for a single 2SC event is thus

$$\Delta E_{\text{LGB}} = \delta_{\text{LGB}} M_{2\text{SC}} c^2, \quad (3)$$

where $M_{2\text{SC}} = \delta_{2\text{SC}} M_{\text{HQS}}$ is the portion of the star in 2SC. Here, $\delta_{2\text{SC}}$ depends on the star's mass while δ_{LGB} represent the portion of the 2SC that is in LGBs (intrinsic property of 2SC; see Ouyed & Sannino 2001). The emission/cooling time is then

$$\Delta t_{\text{cool}} = \frac{\epsilon M_{\text{HQS}} c^2}{L_\gamma}, \quad (4)$$

with $\epsilon = \delta_{2\text{SC}} \delta_{\text{LGB}}$.

4. Powering Gamma-Ray Bursts

4.1. Fireball and baryon loading

The fireball stems from the LGB decay and photon thermalization. The photons are emitted from the star's surface into the vacuum region beneath the inner crust ($\sim 10^3$

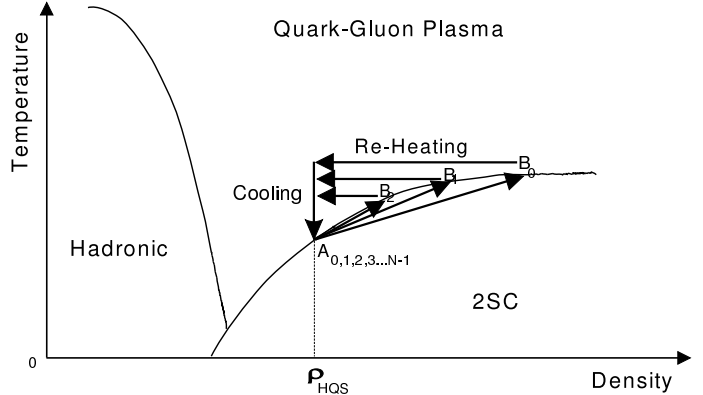


Fig. 2. The episodic emission as illustrated in the QCD phase diagram. The 2SC front spreads deep inside the star and stops at B_0 before re-entering the QGP phase. Following photon cooling, heat flows from the core and re-heats the surface. The star then starts cooling until A_1 is reached at which point the stage is set for the 2SC/LGB/photon process to start all over again ($A_1 \rightarrow B_1$) resulting in another emission.

fm in size). Photon-photon interaction occurs in a much longer time than the vacuum region crossing time. Also, the cross-section for the creation of pairs through interactions with the electrons in the vacuum region is negligible (Rybicki & Lightman 1979; Longair 1992). The fireball energy is thus directly deposited in the crust. If its energy density, aT_c^4 (with a being the radiation density constant), exceeds that of the gravitational energy density in the crust, energy outflow in the form of ions occurs. One can show that the condition

$$aT_c^4 > \frac{GM_{\text{HQS}}}{R_{\text{HQS}}} \rho_{\text{crust}}, \quad (5)$$

where ρ_{crust} is the crust density and G the gravitational constant, is equivalent to

$$\left(\frac{T_c}{30 \text{ MeV}}\right)^4 > \left(\frac{M_{\text{HQS}}}{M_\odot}\right) \left(\frac{5 \text{ km}}{R_{\text{HQS}}}\right) \left(\frac{\rho_{\text{crust}}}{\rho_{\text{drip}}}\right), \quad (6)$$

which is always true if $T_c > 30 \text{ MeV}$. The fireball is thus loaded with nuclei present in the crust. More specifically, it is the energy transfer from photons to electrons which drag the positively charged nuclei in the process. Note that the 2SC layer is not carried out during the two-photon decay process because of the star's high gravitational energy density: $\rho_{\text{HQS}}/\rho_{\text{drip}} \gg 1$.

4.2. Episodic behavior

The star's surface pressure is reduced following photon emission¹. A heat and mass flux is thus triggered from the QGP phase to the 2SC layer re-heating (above T_c) and destroying the superconductive phase. The entire star is

¹ The pressure gradient in the 2SC layer is $\Delta p \propto (8 - 5)T_c^4$ (Farhi & Jaffe 1984) where the massless gluons (3 out of 8) have been consumed by the LGB/photon process.

now in a QGP phase (5 gluons \rightarrow 8 gluons at the surface) and hence the cooling process can start again. This corresponds to the transition $[\rho(\mathbf{B}_0), T(\mathbf{B}_0)] \rightarrow [\rho_{\text{HQS}}, T(\mathbf{B}_0)]$ in the QCD phase diagram (thermal adjustment). The stage is now set for the 2SC/LGB/photon process to start all over again resulting in another emission. For the subsequent emission, however, we expect the system to evolve to point \mathbf{B}_1 generally located at different densities and temperatures than \mathbf{B}_0 (see Fig. 2). The cycle ends after N emissions when $\rho(\mathbf{B}_N) \simeq \rho_{\text{HQS}}$.

The time it takes to consume most of the star (the glue component) by this process is

$$t_{\text{engine}} \simeq \frac{M_{\text{HQS}} c^2}{L_\gamma} \simeq 1 \text{ s} \left(\frac{M_{\text{HQS}}}{M_\odot} \right) \left(\frac{5 \text{ km}}{R_{\text{HQS}}} \right)^2 \left(\frac{30 \text{ MeV}}{T_c} \right)^4, \quad (7)$$

which is representative of the engine's activity. The above assumes quick adjustment of the star following each event, but is not necessarily the case for the most massive stars.

4.3. Multiple shell emission

The episodic behavior of the star together with the resulting loaded fireball (we call shell) offers a natural mechanism for multiple shell emission if $T_c < 30 \text{ MeV}$. Indeed from Eq. (6) a higher T_c value would imply extraction of the entire crust in a single emission and no loading of the subsequent fireballs. Clearly, $T_c < 30 \text{ MeV}$ must be considered if multiple ejections are to occur².

The fraction (f) of the crust extracted in a single event is,

$$\Delta M_{\text{crust}} = f M_{\text{crust}}. \quad (8)$$

The shell is accelerated with the rest of the fireball converting most of the radiation energy into bulk kinetic energy. The corresponding Lorentz factor we estimate to be,

$$\Gamma_{\text{shell}} \simeq \frac{\epsilon M_{\text{HQS}}}{f M_{\text{crust}}}, \quad (9)$$

where we used Eq. (3) and Eq. (8). ϵ and f depend on the star's mass and characterize the two emission regimes in our model.

4.4. Shell-shell collision

The Lorentz factor for the n^{th} shell is

$$\begin{aligned} \Gamma_{\text{shell},n} &= \frac{\epsilon_n M_{\text{HQS},n}}{f_n M_{\text{crust},n}} \\ &= \left(\frac{\epsilon_n}{\epsilon_{n-1}} \right) \left(\frac{f_{n-1}}{f_n} \right) \frac{(1 - \epsilon_{n-1})}{(1 - f_{n-1})} \Gamma_{\text{shell},n-1}. \end{aligned} \quad (10)$$

² Even if T_c turns out to be greater than 30 MeV, in which case the entire crust will be blown away (Eq. (6)), one can imagine mechanisms where crust material is replenished. By accretion, for instance, if the HQS is part of a binary. There are also geometrical considerations where asymmetric emission/ejection can occur due to the rapid rotation of Quark Stars; here only a portion of the crust is extracted at a time. This aspect of the model requires better knowledge of the conditions and environments where HQSs are formed.

The ratio $\Gamma_{\text{shell},n}/\Gamma_{\text{shell},n-1}$ is a function of ϵ (which depends on the details of the cooling process and the spread of the 2SC front) and f (mostly related to the density in the crust). With the two parameters varying from one emission to another, the ratio can be randomly greater or less than 1. As such, the shells will have random Lorentz factors and random energies. Faster shells will catch up with slower ones and will collide, converting some of their kinetic energy to internal energy.

5. The two regimes

When the inner crust density is the neutron drip value, one finds a minimum mass star of $\sim 0.015 M_\odot$. For masses above this critical value, the corresponding crusts are thin and light. They do not exceed few kilometers in thickness. Matter at the density of such crusts is a Coulomb lattice of iron and nickel all the way from the inner edge to the surface of the star (Baym et al. 1971). For masses below $0.015 M_\odot$, the crust can extend up to thousands of kilometers with densities much below the neutron drip. This allows us to identify two distinct emission regimes for a given T_c ($< 30 \text{ MeV}$).

5.1. Light stars ($M_{\text{HQS}} < 0.015 M_\odot$)

These are objects whose average density is $\sim \rho_{\text{HQS}}$ ($M_{\text{HQS}} \simeq \frac{4\pi}{3} R_{\text{HQS}}^3 \rho_{\text{HQS}}$). The 2SC front extends deeper inside the star ($\delta_{2\text{SC}} \sim 1$). The star can be represented by a system close to \mathbf{A}_0 in Fig. 2. Each of the few emissions (defined by ϵ) is thus capable of consuming a big portion of the star. Furthermore, the entire crust material can be extracted in a few 2SC/LGB/photon cycles ($\rho_{\text{crust}}/\rho_{\text{drip}} \ll 1$).

Using Eq. (7), the few emissions lead to

$$\begin{aligned} t_{\text{tot}} &\simeq \text{fraction} \times t_{\text{engine}} \\ &\simeq \text{fraction} \times 0.25 \text{ s} \left(\frac{M_{\text{HQS}}}{0.01 M_\odot} \right) \left(\frac{1 \text{ km}}{R_{\text{HQS}}} \right)^2 \left(\frac{30 \text{ MeV}}{T_c} \right)^4, \end{aligned} \quad (11)$$

where t_{tot} is representative of the observable time which takes into account the presence of the crust.

5.2. Massive stars ($M_{\text{HQS}} \geq 0.015 M_\odot$)

The surface density of a massive star being that of a light star (ρ_{HQS} given by $P = 0$ in Eq. (1)), defines a standard unit in our model. In other words, the mass of the 2SC layer in a massive star case is

$$\Delta M_{2\text{SC},m} \simeq M_{2\text{SC},1}, \quad (12)$$

where “ m ” and “ l ” stand for massive and light, respectively. It implies

$$\frac{\Delta R_{2\text{SC},m}}{R_{2\text{SC},m}} \simeq \frac{1}{3} \left(\frac{R_l}{R_m} \right)^3 \simeq \frac{1}{3} \left(\frac{1 \text{ km}}{5 \text{ km}} \right)^3 \simeq 0.003. \quad (13)$$

For a typical star of 5 km in radius, we then estimate a 2SC layer of about 15 meters thick (much larger than the photon mean free path thus justifying the local thermal equilibrium hypothesis). Equivalently,

$$\bar{\epsilon} = \frac{M_l}{M_m} \simeq \left(\frac{1 \text{ km}}{5 \text{ km}}\right)^3 \simeq 0.01, \quad (14)$$

where $\bar{\epsilon}$ is the average value. This naturally account for many events (or N fireballs). The average number of fireballs with which an entire star is consumed is thus

$$N \simeq \frac{1}{\bar{\epsilon}} \simeq 100. \quad (15)$$

Since most of the crust is at densities close to the neutron drip value, Eq. (6) implies that only a tiny part of the crust surface material (where $\rho_{\text{crust}} \ll \rho_{\text{drip}}$) can be extracted by each of the fireballs. This allows for a continuous loading of the fireballs.

The total observable time in our simplified approach is thus,

$$t_{\text{tot}} \simeq t_{\text{engine}} = 1 \text{ s} \left(\frac{M_{\text{HQS}}}{M_{\odot}}\right) \left(\frac{5 \text{ km}}{R_{\text{HQS}}}\right)^2 \left(\frac{30 \text{ MeV}}{T_c}\right)^4. \quad (16)$$

We isolated two regimes:

(i) Light stars \Rightarrow short emissions.

(ii) Massive stars \Rightarrow long emissions.

It appears, according to BATSE (Burst and Transient Source Experiment detector on the COMPTON-GRO satellite), that the bursts can be classified into two distinct categories (Kouveliotou et al. 1993): short (< 2 s) bursts and long (> 2 s, typically ~ 50 s) bursts. The black body behavior (T_c^4) inherent to our model puts stringent constraints on the value of T_c which best comply with these observations. Using $T_c \simeq 10$ MeV, from Eq. (11) and Eq. (16) we obtain in the star's rest frame

$$t_{\text{tot}} \simeq 81 \text{ s} \left(\frac{M_{\text{HQS}}}{M_{\odot}}\right) \left(\frac{5 \text{ km}}{R_{\text{HQS}}}\right)^2, \quad (17)$$

for massive stars (suggestive of long GRBs), and

$$t_{\text{tot}} \simeq 2 \text{ s} \left(\frac{M_{\text{HQS}}}{0.01 M_{\odot}}\right) \left(\frac{1 \text{ km}}{R_{\text{HQS}}}\right)^2, \quad (18)$$

for light stars (suggestive of short GRBs). There is a clear correlation (almost one to one) between the observed burst time and the time at which the source ejected the specific shell (see Figure 3 in Kobayashi et al. 1997, for example). Note that $T_c \simeq 10$ MeV implies that only a portion of the crust is extracted. This is also consistent with our previous assumption ($T_c < 30$ MeV) and subsequent calculations.

When $T_c \simeq 10$ MeV, Eq. (6) gives $\rho_{\text{crust}}/\rho_{\text{drip}} \simeq 1/16$. For an appropriate crust density profile (using the equation of state given in Baym et al. 1971), from Eq. (8) we find $\bar{f} \simeq 0.01$. This implies (making use of Eq. (14))

$$\Gamma_{\text{shell}} = 2 \times 10^5 \left(\frac{\epsilon}{0.01}\right) \left(\frac{0.01}{f}\right). \quad (19)$$

For massive stars then³

$$0 < \Gamma_{\text{shell}} < 2 \times 10^5. \quad (20)$$

For light stars, where both ϵ and f are close to unity, $\Gamma_{\text{shell}} \simeq 10^5$. The shells are also heavier than in the massive stars case. We thus expect stronger shocks from the shell-shell collision resulting in harder bursts. Combined with our previous results, this is suggestive of

(i) Light stars \Rightarrow short and hard bursts.

(ii) Massive stars \Rightarrow long and soft bursts.

Eq. (17) and Eq. (18) is simply Eq. (7) rescaled to the appropriate object size. We separated two regimes due to intrinsic differences in the engine and the crust. From the engine point of view, massive stars generate many more emissions when compared to light ones, and no substantial reduction of the engine time is expected because of the omni-presence of the crust. Another important difference is related to the physics of the multiple re-adjustments following each event which is more pronounced for very massive stars. The latter among other factors is related to ϵ which can vary from one event to another.

6. Features and predictions

6.1. GRB energies

The maximum available energy is when the heaviest HQS ($M_{\text{HQS,max}} \simeq 2M_{\odot}$) is entirely consumed. That is,

$$E_{\text{LGB,max}} \simeq 4 \times 10^{54} \text{ ergs}. \quad (21)$$

The corresponding GRB energy is

$$E_{\text{GRB,max}} \simeq 1.6 \times 10^{54} \text{ ergs}, \quad (22)$$

where we used a fiducial conversion efficiency of 40% (Sect. 6.4).

Since $M_{\text{HQS,min}} < 0.015M_{\odot}$ we conclude that,

$$E_{\text{LGB,min}} < 3 \times 10^{52} \text{ ergs}, \quad (23)$$

implying

$$E_{\text{GRB,min}} < 1.2 \times 10^{52} \text{ ergs}. \quad (24)$$

6.2. GRB total duration

From Eq. (17) and Eq. (18) we have

$$t_{\text{tot}} \simeq 81 \text{ s}, \quad (25)$$

for typical massive stars, and

$$t_{\text{tot}} \simeq 2 \text{ s}, \quad (26)$$

³ Note that a *relativistic loaded fireball* is not necessarily achieved since $\Gamma_{\text{shell}} < 100$ at times. Gaps in the GRBs spectra are thus expected according to our model.

for typical light stars.

Our estimate of the duration time for the massive star case should be taken as a lower limit. As we have said, a complete model should take into account star readjustments. Nevertheless, we can still account for a wide range in GRB duration by an appropriate choice of different values of the mass and radius.

6.3. Peak duration vs energy

The peak duration (t_p) is related to the time measured by a clock on the shell via (Fenimore & Ramirez-Ruiz 1999),

$$t_p \simeq \frac{t_{\text{shell}}}{2\Gamma_{\text{shell}}} = \frac{1}{2\Gamma_{\text{shell}}} \times \frac{\Delta X_{\text{shell}}}{c_s}, \quad (27)$$

where c_s is the speed of the shock front crossing the shell leading to the burst. We find

$$t_p \simeq \frac{1}{c_s} \times \frac{\epsilon M_{\text{HQS}}}{4\pi R_{\text{HQS}}^2 \rho_{\text{crust}}}. \quad (28)$$

In the above we used Eq. (9) and $M_{\text{shell}} = \Delta M_{\text{crust}} = 4\pi R_{\text{crust}}^2 \Delta X_{\text{crust}} \rho_{\text{crust}}$. The expression on the right is $\propto \Delta t_{\text{cool}}$ as can be seen from Eq. (4) and in our model is constant for a given star. The only parameter which is directly linked to the shell dynamics and energetics is c_s . Shock physics gives (Ouyed & Pudritz 1993)

$$c_s^2 \propto E_{\text{int.}}, \quad (29)$$

where $E_{\text{int.}}$ is the shell's internal energy gained during the collision observed as the peak's energy (E_p). That is,

$$t_p \propto E_p^{-0.5}, \quad (30)$$

in reasonable agreement with the power law dependence extracted from temporal vs energy structure in GRBs (index that is between -0.37 and -0.46 ; Fenimore et al. 1995).

6.4. Shell dynamics

Take a shell of thickness ΔX_{crust} to be extracted from the crust. The upper surface of the shell is extracted first while its lower surface lags behind by $(c - v_{\text{shell}})t \simeq ct/(2\Gamma_{\text{shell}}^2)$ (t is the time to eject the entire shell in the star's rest frame). Taking into account mass conservation and the fact that $\Delta X_{\text{shell}} = 2\Gamma_{\text{shell}}^2 \Delta X_{\text{crust}}$, it is straightforward to show

$$\rho_{\text{shell}} \propto \frac{1}{\Gamma_{\text{shell}}^2}. \quad (31)$$

Interestingly enough, these are the required conditions (including the result from Eq. (20)) in the internal shock model which lead to the highest (up to 40%) conversion efficiency and the most desirable temporal structure (Kobayashi et al. 1997; Mochkovitch et al. 1995).

7. Discussion and Conclusion

7.1. Existence and formation of quark stars

In the last few years, thanks to the large amount of fresh observational data collected by the new generation of X-ray and γ -ray satellites, new observations suggest that the compact objects associated with the X-ray pulsars, the X-ray bursters, particularly the SAX J1808.4-3658, are good quark stars candidates (see Li et al. 1999). While these observations/measurements are hints that such objects might exist in nature it remains to explain their formation. More importantly to our model, the bimodal mass distribution remains to be explained.

7.1.1. Massive stars

For the massive stars the conversion of neutron stars to quark stars is one plausible scenario (Cheng & Dai 1996; Ma 1996; Bombaci & Datta 2000). They could also form via the direct mechanism following a supernova collapse where the core collapsed to a stable quark matter instead of neutron matter (Gentile et al. 1993; Dai et al. 1995). Both mechanisms would lead to the formation of quark stars (strange stars to be more specific) with masses in the solar mass range.

7.1.2. Light stars

The formation of small quark stars has already been discussed (early discussions can be found in Alpar 1987; Glendenning et al. 1995; see also Chapter 10.5 in Glendenning 1997) although these remain less understood than the massive ones. In the case of 4U 1728-34 (where a mass of much less than $1.0M_{\odot}$ was derived; Bombaci 1999), it seems that accretion-induced collapse of white dwarfs is a favored formation mechanism. If the quark star formed via the direct conversion mechanism then it required too much mass (at least $\sim 0.8M_{\odot}$ to be ejected during the conversion).

How and why stars in the $0.01M_{\odot}$ range would form remains to be explained. Our arguments were solely based on theoretical considerations related to the critical density in the inner crust (neutron drip) as to differentiate between small stars with thick and heavy crust versus stars with thinner and lighter crusts.

7.2. Neutrino cooling and HQSs

If neutrino cooling is shown to remain efficient in the 2SC phase (for comparison of cooling paths between quark stars and neutron stars and the plausible effects of 2SC on cooling we refer the interested reader to Schaab et al. 1997; Blaschke et al. 2000; Blaschke et al. 2001), we would be left with the scenario where the entire HQS enters the 2SC phase, in which case the 2SC/LGB/photon process (the fireball) occurs only once and inside the entire star. Here, one must involve more complicated physics (such as

that of the crust) to account for the episodic emissions so crucial to any model of GRBs. It is not clear at the moment how to achieve this and is left as an avenue for future research.

7.3. 2SC-II stars

The 2SC/LGB/photon process might proceed until one is left with an object made entirely of 2SC. We name such objects *2SC-II* stars⁴ which are still bound by strong interactions (their density is constant $\sim \rho_{\text{HQS}}$). 2SC-II stars carry an Iron/Nickel crust left over from the GRB phase. The crust mass range is $0 < M_{2\text{SC,crust}} < 5 \times 10^{-5} M_{\odot}$ depending on the efficiency of crust extraction/ejection during the GRB phase.

BATSE observes on average one burst per day. This corresponds, with the simplest model - assuming no cosmic evolution of the rate - to about once per million years in a galaxy (Piran 1999a). In the Milky way we thus expect up to 10^5 of 2SC-II stars. Nevertheless, they are tiny enough ($M \leq 10^{-2} M_{\odot}$, $R \leq 1$ km) to be difficult to detect.

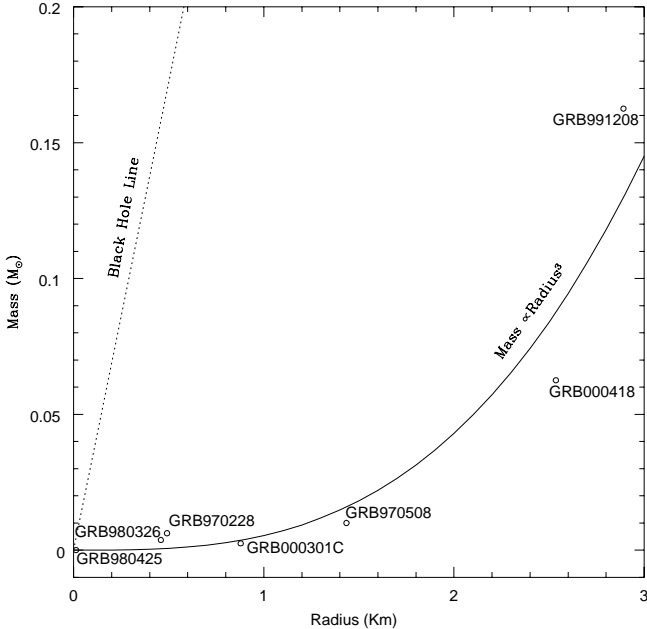


Fig. 3. The Mass–Radius plane derived in our model using few existing GRBs with known energies and total duration. The solid curve shows the $M_{\text{HQS}} = \frac{4\pi}{3} \rho_{\text{HQS}} R_{\text{HQS}}^3$ equation for $\rho_{\text{HQS}} \simeq 9\rho_{\text{N}}$.

⁴ The “II” in 2SC is a simple reminder of the final state of the star, namely the 2SC with only 5 gluons.

7.4. The Mass–Radius Plane

Take observed GRBs with known energies and total duration. From the burst total energy $E_{\text{GRB}} \simeq 0.4Mc^2$ we derive the mass while the burst total duration (t_{tot}) gives us the radius (using Eq. (16) with $T_c \simeq 10$ MeV). In Fig. 3 we plot the resulting Mass–Radius. Note that while neutron stars, can only exist above a certain mass ($\sim 0.1M_{\odot}$; Baym et al. 1971), there is no lower limit to the mass of quark stars. These would be bound by the strong interaction even in the absence of gravity.

The solid curve shows the $M_{\text{HQS}} = \frac{4\pi}{3} \rho_{\text{HQS}} R_{\text{HQS}}^3$ equation which is a reasonable approximation for quark stars. While the GRB data set used is limited nevertheless it seems to support the idea that extremely compact objects ($M \propto R^3$) are behind GRBs activity within our model.

Acknowledgements. The authors thank J. Schechter, K. Rajagopal, I. Bombaci, and F. Weber for interesting and helpful discussions.

References

- Alcock, C., Farhi, E., & Olinto, A. 1986, ApJ, 310, 261
 Alpar, A. M. 1987, Phys. Rev. Lett, 58, 2152
 Baym, G., Pethick, C. J., & Sutherland, P. G. 1971, ApJ, 170, 299
 Blandford, R. D., & Znajek, R. L. 1977, MNRAS, 179, 433
 Blaschke, D., Klähn, T., & Voskresensky, D. N. 2000, ApJ, 533, 406
 Blaschke, D., Grigorian, H., & Voskresensky, D. N. 2001, A&A, 368, 561
 Bodmer, A. R. 1971, Phys. Rev. D, 4, 1601
 Bombaci, I., & Datta, B. 2000, ApJ, 530, L69
 Carter, G. W., & Reddy, S. (hep-ph/0005228)
 Cheng, K. S., & Dai, Z. G. 1996, Phys. Rev. Lett., 77, 1210
 Dey, M., Bombaci, I., Dey, J., Ray, S., & Samanta, B. C. 1998, Phys. Lett. B, 438, 123
 Eichler, D., Livio, M., Piran, T. & Schramm, D. N. 1989, Nature, 340, 126
 Farhi, E., & Jaffe, R. L. 1984, Phys. Rev. D, 30, 2379
 Fenimore, E. E. et al. 1995, ApJ, 448, L101
 Fenimore, E. E., & Ramirez-Ruiz, E. 1999, in Gamma-Ray Bursts: The first three minutes, ASP Conference Series, Vol. 190, eds. J. Poutanen and R. Svensson, p67
 Glendenning, N. K., & Weber, F. 1992, ApJ, 400, 647
 Glendenning, N. K., Kettner, Ch., & Weber, F. 1995, Phys. Rev. Lett., 74, 18, 3519
 Glendenning, N. K. 1997, Compact stars (Springer)
 Goodman, J. 1986, ApJ, 308, L47
 Haensel, P., Zdunik, J. L., & Schaefer, R. 1986 A&A, 160, 121
 Hong, D. K., Hsu, S. D. H., & Sannino, F. 2001, Phys. Lett. B, 516, 362
 Janka, H. -T., Eberl, T., Ruffert, M., & Fryer, C. 1999, ApJ, 527, L39
 Kobayashi, S., Piran, T. & Sari, R. 1997, ApJ, 490, 92
 Kouveliotou, C., Meegan, C. A., Fishman, G. J., et al. 1993, ApJL, 413, L101
 Kouveliotou, C., Briggs, M. S., & Fishman, G. J., (Eds), Gamma Ray Bursts, AIP Conf. Proc., 384 (AIP, New York, 1995)
 Kulkarni, S. R., et al. 1999, Nature, 398, 389

- Li, X. -D, et al. 1999, Phys. Rev. Lett., 83, 3776
- Longair, M. S. 1992, High energy astrophysics (Cambridge Univ. Press)
- Ma, F. 1996, ApJ, 462, L63
- Mochkovitch, R., Maitia, V., & Marques, R. 1995, pJ, 462, L63
in Towards the Source of Gamma-Ray Bursts, Proceedings of 29th ESLAB Symposium, ed. K. Bennet & C. Winkler, 531
- Olinto, A. 1987, Phys. Lett. B, 192, 71
- Ouyed, R. & Pudritz, R. E. 1993, ApJ, 419, 255
- Ouyed, R. 2002, in Compact Stars in the QCD Phase Diagram, Proceedings (astro-ph/0201408)
- Ouyed, R., & Sannino, F. 2001, Phys. Lett. B. 511, 66
- Ouyed, R., Dey, J., & Dey, M. (astro-ph/0105109)
- Paczynski, B. 1990, ApJ, 363, 218
- Piran, T. 1999a, Phys. Rev., 314, 575
- Piran, T. 1999b, in Gamma-Ray Bursts: The first three minutes, ASP Conference Series, Vol. 190, eds. J. Poutanen and R. Svensson, p3
- Rajagopal, K. & Wilczek, F. (hep-ph/0011333)
- Ruffert, M., & Janka, H. -T. 1999, A&A, 344, 573
- Rybicki, G. B. 1979, & Lightman, A. P. Radiative processes in astrophysics (Wiley)
- Sannino, F. 2002, in Compact Stars in the QCD Phase Diagram, Proceedings (hep-ph/0112029)
- Schaab, C., Hermann, B., Weber, F., & Manfred, K. 2000, ApJ, 480, L111
- Shemi, A., & Piran, T. 1990, ApJ, 365, L55
- Witten, E. 1984, Phys. Rev. D, 30, 272